NIH Public Access
Author Manuscript
Biochemistry. Author manuscript; available in PMC 2009 August 26.

Published in final edited form as:
Biochemistry. 2008 August 26; 47(34): 9007–9015. doi:10.1021/bi800419e.

Kinetic and Spectroscopic Studies of the ATP:Corrinoid Adenosyltransferase PduO from *Lactobacillus reuteri*: Substrate Specificity and Insights into the mechanism of Co(II)corrinoid Reduction†

Kiyoung Park†, **Paola E. Mera**‡, **Jorge C. Escalante-Semerena**‡, and **Thomas C. Brunold***,†

† *University of Wisconsin-Madison, Department of Chemistry, Madison, Wisconsin 53706*

‡ *University of Wisconsin-Madison, Department of Bacteriology, Madison, Wisconsin 53706*

Abstract

The PduO-type ATP:corrinoid adenosyltransferase from *Lactobacillus reuteri* (*Lr*PduO) catalyzes the formation of the essential Co–C bond of adenosylcobalamin (coenzyme B_{12}) by transferring the adenosyl group from co-substrate ATP to a transient Co^{1+}corrinoid species generated in the enzyme active site. While PduO-type enzymes have previously been believed to be capable of adenosylating only Co^{1+}cobalamin ($Co^{1+}Cbl^{-}$), our kinetic data obtained in this study provide *in vitro* evidence that *Lr*PduO can in fact also utilize the incomplete corrinoid Co^{1+}cobinamide (Co^{1+}Cbi) as an alternative substrate. To explore the mechanism by which *Lr*PduO overcomes the thermodynamically challenging reduction of its Co^{2+}corrinoid substrates, we have examined how the enzyme active site alters the geometric and electronic properties of Co^{2+}Cbl and $Co^{2+}Cbi^{+}$ by using electronic absorption, magnetic circular dichroism, and electron paramagnetic resonance spectroscopic techniques. Our data reveal that upon binding to *Lr*PduO that was pre-incubated with ATP, both Co^{2+}corrinoids undergo a partial (~40–50%) conversion to distinct paramagnetic Co^{2+}species. The spectroscopic signatures of these species are consistent with essentially four-coordinate, square-planar Co^{2+} complexes, based on a comparison with the results obtained in our previous studies of related enzymes. Consequently, it appears that the general strategy employed by adenosyltransferases for effecting $Co^{2+}\rightarrow Co^{1+}$ reduction involves the formation of an "activated" Co^{2+}corrinoid intermediate that lacks any significant axial bonding interactions, so as to stabilize the redox-active, Co $3d_{z^2}$-based molecular orbital.

Coenzyme B_{12}, which is also known as adenosylcobalamin (AdoCbl[1]), provides one of very few known examples of a bio-organometallic species (1). AdoCbl contains a cobalt(III) ion that is equatorially ligated by four nitrogens of a tetrapyrrole macrocycle, termed the corrin ring, and axially coordinated by the 5′-carbon atom of an adenosyl (Ado) moiety on the "upper" face and a nitrogen atom from 5,6-dimethylimidazole (DMB) on the "lower" face (Figure 1) (2). The DMB is part of a nucleotide loop that is tethered to the corrin ring at C^{17}; in

†This work was supported in part by the National Science Foundation grant MCB-0238530 (to T.C.B.) and the National Institutes of Health grant R01-GM40313 (to J.C.E.-S.). P.E.M was supported in part by National Research Service Award 5F31GM081979-02 from the National Institute of General Medical Sciences (NIGMS).

*Corresponding author: Thomas C. Brunold, Department of Chemistry, 1101 University Ave., Madison, WI 53706; phone, (608) 265-9056; fax, (608) 262-6143, AUTHOR EMAIL ADDRESS: brunold@chem.wisc.edu.

[1]Abbreviations: Abs, electronic absorption; AdoCbl, adenosylcobalamin; $AdoCbi^{+}$, adenosylcobinamide; H_2OCbl^{+}, aquacobalamin; Cbl, cobalamin; cbi, cobinamide; CNCbl, cyanocobalamin; $(H_2O)_2Cbi^{2+}$, diaquacobinamide; $(CN)_2$Cbi, dicyanocobinamide; DMB, dimethylbenzimidazole; EPR, electron paramagnetic resonance; hATR, human adenosyltransferase; *Lr*PduO, *Lactobacillus reuteri* PduO; MCD, magnetic circular dichroism; $NaBH_4$, sodium borohydride.

NIH-PA Author Manuscript
NIH-PA Author Manuscript
NIH-PA Author Manuscript

NIH-PA Author Manuscript

NIH-PA Author Manuscript

NIH-PA Author Manuscript

adeonsylcobinamide ($AdoCbi^+$), this loop is absent and the lower axial coordination site is occupied by a water molecule to complete a distorted octahedral ligand environment of the Co^{3+} ion (3).

AdoCbl serves as a cofactor for numerous distinct enzymes that catalyze radical-induced rearrangement reactions (4–10), such as methylmalonyl-CoA mutase, glutamate mutase, diol dehydratase, and ethanolamine ammonia lyase, or ribonucleotide reduction, as exemplified by the ribonucleotide tri-phosphate reductase (11). Common to these enzymes is that the first step in their respective catalytic cycles involves homolytic cleavage of the cofactor's Co–C bond to yield Co^{2+}cobalamin (Co^{2+}Cbl) and an organic radical centered on the 5′-carbon of the Ado moiety. The Ado• radical generated in this process then abstracts a hydrogen atom from substrate to initiate a protein-mediated rearrangement reaction that eventually leads to product formation and regeneration of the AdoCbl cofactor (12–14).

Eukaryotes lack the biosynthetic machinery needed to synthesize AdoCbl *de novo*. Instead, those eukaryotes that utilize AdoCbl in their metabolism (which does not include plants) convert exogenous cobalamins, such as vitamin B_{12} (in which the upper axial coordination site is occupied by a CN^- moiety rather than Ado), to AdoCbl by using a class of enzymes termed adenosyltransferases (15,16). The importance of these enzymes is highlighted by the fact that the malfunctioning of the human adenosyltransferase (hATR) can cause methylmalonic aciduria, an autosomal disorder that is often fatal in infants (17). Many prokaryotes also require AdoCbl; e.g., for the utilization of propanediol and ethanolamine to produce substrates for ATP production and as sources of carbon and nitrogen, respectively (7,8). Some of these organisms are capable of synthesizing AdoCbl *de novo* in a process involving over 25 enzymes, which catalyze the stepwise conversion of 5-aminolevulinic acid to the complete cofactor via an intermediate named cobyric acid, a cobalamin precursor that possesses all of the necessary functionality except for the nucleotide loop and the axial Ado ligand (18).

Regardless of whether an organism synthesizes AdoCbl *de novo* or salvages incomplete corrinoids from its environment, both processes require two one-electron reduction steps to convert Co^{3+} to Co^{1+} and the formation of the essential Co–C bond by transferring the Ado group from a molecule of ATP to the transiently formed Co^{1+}corrinoid species (19,20). While previous studies revealed that the $Co^{3+/2+}$corrinoid reduction potential is sufficiently positive to ensure that the Co^{3+}corrinoid be converted to the Co^{2+} state in the reducing environment of the cytoplasm (21), the $Co^{2+/1+}$corrinoid potential is lower than the midpoint potentials of putative *in vivo* reducing agents. For example, the $Co^{2+/1+}$ reduction potential of aqueous Co^{2+}Cbl ($E° = -610$ mV) is well below that of the semiquinone/reduced flavin couple of flavodoxin A (FldA, $E° = -440$ mV) (22–24). Despite this apparent thermodynamic dilemma, it has been shown that in the presence of adenosyltransferases, the $Co^{2+} \rightarrow Co^{1+}$ reduction can be effected under physiologically relevant conditions (25–27).

Previously, our spectroscopic and computational studies of two representative members of the family of adenosyltransferases, CobA from *Salmonella enterica* and hATR, have provided definitive clues as to how these enzymes overcome the thermodynamically challenging task of reducing Co^{2+}corrinoids to their Co^{1+} oxidation state (28,29). Specifically, we have shown that upon binding of Co^{2+}cobinamide ($Co^{2+}Cbi^+$) to CobA complexed with co-substrate ATP, the axially bound water molecule (partially) dissociates so as to generate an effectively four-coordinate square-planar Co^{2+} species. As a result of this (partial) ligand dissociation, the redox-active Co $3d_z2$ orbital that is oriented toward the axial coordination sites is significantly stabilized in energy, thereby raising the $Co^{2+/1+}$ reduction midpoint potential by an estimated 250 mV (28). Remarkably, the same spectroscopic signatures characterizing this "activated" four-coordinate Co^{2+} species features have been found to develop upon binding of Co^{2+}Cbl

NIH-PA Author Manuscript

NIH-PA Author Manuscript

NIH-PA Author Manuscript

to hATR in the presence of ATP (29), even though hATR and CobA are structurally and evolutionary unrelated (7,30,31).

Recently, St. Maurice et al. have purified an hATR-type adenosyltransferase from *Lactobacillus reuteri*, termed *Lr*PduO, and reported its X-ray crystal structure with ATP bound to the active site (32). *In vivo* and *in vitro* experiments have confirmed that *Lr*PduO can convert $Co^{1+}Cbl^{-}$ to AdoCbl and revealed that it can substitute for CobA in *Salmonella enterica*, implying that *Lr*PduO possesses the ability to adenosylate both Co^{2+}Cbl and $Co^{2+}Cbi^{+}$ (16, 32). In the present study, we have performed a detailed kinetic and spectroscopic characterization of *Lr*PduO to obtain molecular-level insight into certain steps of the catalytic mechanism employed by this enzyme. Our kinetic parameters obtained for the reaction of Co^{1+}Cbi with *Lr*PduO/ATP confirm that cobinamide can serve as an alternative substrate for this adenosyltransferase, while our spectroscopic data indicate that *Lr*PduO utilizes the same general strategy for promoting $Co^{2+}\rightarrow Co^{1+}$ reduction as CobA and hATR; namely, to generate an effectively four-coordinate Co^{2+}corrinoid species regardless of whether Co^{2+}Cbl or $Co^{2+}Cbi^{+}$ is used as the substrate. Nonetheless, a comparison of the results obtained for *Lr*PduO and those reported previously for hATR and CobA reveals small but notable differences with regards to the substrate specificity and degree of Co^{2+}corrinoid activation.

MATERIALS AND METHODS

Cofactors and Chemicals

Aquacobalamin (H_2OCbl^{+}), dicyanocobinamide ($(CN)_2Cbi$), and sodium borohydride ($NaBH_4$) were purchased from Sigma and used as obtained. Diaquacobinamide ($(H_2O)_2Cbi^{2+}$) was prepared by reducing $(CN)_2Cbi$ with $NaBH_4$, loading the reaction mixture on a C18 SepPack column, washing with doubly distilled H_2O, and eluting the product with methanol, as described in a previous report (28). Co^{2+}Cbl and $Co^{2+}Cbi^{+}$ were prepared by adding $NaBH_4$ to degassed aqueous solutions of H_2OCbl^{+} and $(H_2O)_2Cbi^{2+}$, respectively, in the presence of 60% (v/v) glycerol, and the progress of the conversion was monitored spectrophotometrically.

Protein Production and Purification

Recombinant PduO protein from *Lactobacillus reuteri* was obtained by overexpressing a pTEV3 plasmid transformed into *Escherichia coli* strain BL21(DE3). pTEV3 encodes the *Lr*PduO protein with an N-terminal $(His)_6$ tag (32,33). This $(His)_6$ tag was subsequently clipped off using rTEV protease, and the tag-free enzyme was purified using a HisTrap FF column (Amersham Biosciences), as described previously (32). Purified *Lr*PduO was stored at −80 °C in Tris-HCl buffer (0.1 M, pH 8 at 4 °C) containing NaCl (0.5 M). Protein samples used for kinetic analyses additionally contained 10% (v/v) glycerol.

Kinetic Studies

Activity assays were performed as described previously (32) without modifications (final *Lr*PduO concentration was 1 μg/mL). $AdoCbi^{+}$ formation was monitored spectrophotometrically at 388 nm, which corresponds to the peak position of the dominant absorption feature of Co^{1+}Cbi. The values of V_{max} and K_m were determined from plots of the initial velocity versus substrate concentration. All kinetic parameters were determined in duplicates; their values and uncertainties as reported in this paper correspond to the average of the two measurements and their standard deviations, respectively.

NIH-PA Author Manuscript

NIH-PA Author Manuscript

NIH-PA Author Manuscript

Sample Preparation

Solutions of *Lr*PduO (in 50 mM Tris-HCl buffer, pH 8 containing 0.5 M NaCl) in the absence or presence of 3 mM MgATP were purged separately with Ar gas for 30 min at 4 °C before they were combined with the degassed free Co^{2+}corrinoid solutions in a 0.9:1.0 Co^{2+}corrinoid:*Lr*PduO molar ratio in a sealed anaerobic vial (final enzyme concentration of 0.4 mM). The reaction mixtures, which contained 60% (v/v) glycerol, were then transferred anaerobically into the appropriate sample cells (previously purged with Ar gas) and immediately frozen in liquid N_2.

Spectroscopy

Low-temperature electronic absorption (Abs) and magnetic circular dichroism (MCD) spectra were collected on a Jasco J-715 spectropolarimeter in conjunction with an Oxford Instruments SM-4000 8T magnetocryostat. All MCD spectra presented in this paper were obtained by taking the difference between spectra collected with the magnetic field oriented parallel and antiparallel to the light propagation axis to remove contributions from the natural CD and glass strain.

X-band EPR spectra were obtained by using a Bruker ESP 300E spectrometer in conjunction with an Oxford ESR 900 continuous flow liquid helium cryostat and an Oxford ITC4 temperature controller. The microwave frequency was measured with a Varian EIP model 625A CW frequency counter. All spectra were collected using a modulation amplitude of 10 G, a modulation frequency of 100 kHz, and a time constant of 41 ms. EPR spectral simulations were performed using the WEPR program developed by Dr. Frank Neese (34).

RESULTS AND ANALYSIS

Kinetic Studies

To explore whether *Lr*PduO possesses the ability to adenosylate incompletely assembled corrinoids in addition to $Co^{1+}Cbl^{-}$ (32), initial velocity kinetic measurements were performed using chemically reduced Co^{1+}Cbi as the substrate. In these experiments, the concentration of Co^{1+}Cbi was varied while that of the co-substrate ATP was kept at saturation. The apparent K_m for Co^{1+}Cbi (K_m = 0.096 μM) was found to be similar to the one reported for $Co^{1+}Cbl^{-}$ (K_m = 0.13 μM). Likewise, the rates at which *Lr*PduO can adenosylate $Co^{1+}Cbl^{-}$ and Co^{1+}Cbi are nearly indistinguishable (k_{cat} = 2.0 and 2.4 × 10^{-2} s^{-1}, respectively, see Table 1), indicating that, at least *in vitro*, the nucleotide loop is not required for the binding and adenosylation of the corrinoid substrate by *Lr*PduO.

Co^{2+}Cbl ↔ LrPduO Interactions

(A) Co^{2+}Cbl + LrPduO—The low-temperature Abs spectra of Co^{2+}Cbl in the absence and presence of *Lr*PduO are nearly identical with respect to band positions and intensities (cf Figures 2A and 2B). Although the addition of *Lr*PduO causes a minor blue-shift of the prominent feature in the visible spectral region (the α-band (35)) of the Co^{2+}Cbl Abs spectrum, from 21010 to 21050 cm^{-1} (Table 2), it has no discernible effect on the position of the dominant Abs feature in the near-UV region at ~32150 cm^{-1} (note that the shoulder near 18520 cm^{-1} in the Co^{2+}Cbl + *Lr*PduO Abs spectrum is due to the presence of a small fraction of re-oxidized corrinoid in that sample).

A complementary and considerably more sensitive probe of the interaction between Co^{2+}Cbl and *Lr*PduO is provided by low-temperature MCD spectroscopy. Because the low-energy region of the Co^{2+}corrinoid MCD spectra is dominated by ligand-field (LF) transitions, this region is particularly valuable for monitoring changes in the Co^{2+} coordination environment (35). Hence, the fact that the MCD spectra of Co^{2+}Cbl in the absence and presence of *Lr*PduO

NIH-PA Author Manuscript

NIH-PA Author Manuscript

NIH-PA Author Manuscript

are virtually identical (cf Figures 2A and 2B) rules out any major structural perturbations to the Co^{2+} center upon cofactor binding to the enzyme active site.

Consistent with our MCD results, the EPR spectra of Co^{2+}Cbl in the absence and presence of *Lr*PduO are nearly superimposable (cf Figures 3A and 3B). However, closer examination of the EPR spectrum of Co^{2+}Cbl + *Lr*PduO reveals the presence of a broad feature near 2600 G that has no counterpart in the spectrum of the free cofactor. This feature is characteristic of base-off Co^{2+}Cbl (36, 37), a species in which a water molecule binds to the lower axial coordination site of the Co^{2+} center that was originally occupied by the DMB moiety in base-on Co^{2+}Cbl (Figure 1). A quantitative analysis of the Co^{2+}Cbl + *Lr*PduO EPR spectrum reveals that this sample contains ~30% base-off Co^{2+}Cbl. This finding correlates nicely with the slight blue-shift of the α-band that is observed in the Co^{2+}Cbl Abs spectrum upon the addition of *Lr*PduO (Figures 2A and 2B, Table 2). The *g* and ^{59}Co hyperfine values *A*(Co) obtained from simulations of the EPR spectra presented in Figure 3 are summarized in Table 3.

(B) Co^{2+}Cbl + LrPduO/ATP—While the spectral changes in response to Co^{2+}Cbl binding to substrate-free *Lr*PduO are quite modest (see above), a rather significant blue-shift of the α-band is observed in the Abs spectrum of Co^{2+}Cbl upon the addition of the *Lr*PduO complexed with the co-substrate ATP (cf Figures 2B and 2C, Table 2). This shift occurs in parallel with a dramatic change to the MCD spectrum, most notably the appearance of new features at ~12340 and 20580 cm^{-1} (Figure 2C). Because the MCD feature at 12340 cm^{-1} has no discernible counterpart in the Abs spectrum, it can be attributed to a magnetic-dipole allowed Co^{2+} d→d transition (38, 39). An analogous low-energy MCD feature has been observed for Co^{2+}Cbl bound to the hATR/ATP complex, where it was shown to reflect the presence of an effectively four-coordinate Co^{2+}Cbl species (29). Our MCD data thus provide compelling evidence that a four-coordinate Co^{2+}Cbl species is also formed when Co^{2+}Cbl binds to the *Lr*PduO/ATP complex. This conversion is not complete, however, as the negative features at 15250 and 16880 cm^{-1} and the positive features at 18000 and 18850 cm^{-1} in the MCD spectrum of Co^{2+}Cbl + *Lr*PduO/ATP (Figure 2C) are characteristic of base-on Co^{2+}Cbl (see Figure 2A). This fraction of five-coordinate Co^{2+}Cbl corresponds to either unbound corrinoid substrate or to an enzyme-bound species that has resisted conversion to the four-coordinate form.

In agreement with our MCD data presented in Figure 2, the EPR spectrum of Co^{2+}Cbl + *Lr*PduO/ATP (Figure 3C) reveals the presence of at least two distinct paramagnetic species, one exhibiting an EPR spectrum characteristic of base-on Co^{2+}Cbl (see Figure 3A) and the other giving rise to the appearance of a series of widely spread resonances in the low-field region. To better resolve the features associated with the latter species, the suitably scaled (×0.6) Co^{2+}Cbl + *Lr*PduO EPR spectrum (Figure 3B) was subtracted from the composite spectrum in Figure 3C to obtain the trace shown in Figure 3D. As expected on the basis of our MCD data analysis (vide supra), the resulting spectrum is very similar to that reported for the four-coordinate Co^{2+}Cbl species in samples of Co^{2+}Cbl + hATR/ATP (29). In particular, the $g_{2,3}$ and *A*(Co) values obtained from a fit of the EPR spectrum in Figure 3D are much larger than those of any five-coordinate Co^{2+}Cbl species (Table 3), and are instead characteristic of an essentially square-planar Co^{2+} complex that lacks any significant axial bonding interactions (28,40,41).

$Co^{2+}Cbi^{+}$ ↔ LrPduO Interactions

(A) $Co^{2+}Cbi^{+}$ + LrPduO—The low-temperature Abs and MCD spectra of $Co^{2+}Cbi^{+}$ in the absence and presence of *Lr*PduO are very similar to each other (cf Figures 4A and 4B). However, while the addition of *Lr*PduO to the $Co^{2+}Cbi^{+}$ solution has no effect on the peak position of the α-band (Table 2), it causes a small but notable broadening of several features in the 16000 – 21000 cm^{-1} region of the MCD spectrum. Similarly, the EPR spectrum of

NIH-PA Author Manuscript

NIH-PA Author Manuscript

NIH-PA Author Manuscript

$Co^{2+}Cbi^{+}$ is slightly perturbed when *Lr*PduO is present, especially between 2800 and 3100 G (cf Figures 5A and 5B). Collectively, these data suggest that $Co^{2+}Cbi^{+}$ binds to *Lr*PduO even in the absence of co-substrate ATP, but retains a five-coordinate Co^{2+} center with an axially bound water molecule. Interestingly, our simulation of the $Co^{2+}Cbi^{+}$+ *Lr*PduO EPR spectrum reveals that $g_2 \neq g_3$ for this species, indicating that the Co^{2+} ion is in a ligand environment of rhombic symmetry, while for free $Co^{2+}Cbi^{+}$ an axially symmetric spectrum with $g_2 = g_3$ is observed (see Table 3).

(B) $Co^{2+}Cbi^{+}$ + LrPduO/ATP—As in the case of Co^{2+}Cbl + *Lr*PduO/ATP (Figure 2), a significant blue-shift of the α-band (Table 2) and the appearance of prominent MCD features at 12310 and 20530 cm^{-1} are observed when $Co^{2+}Cbi^{+}$ is incubated with *Lr*PduO complexed with the co-substrate ATP (cf Figures 4A and 4C). Again, the conversion to a four-coordinate Co^{2+}corrinoid species is incomplete, based on the observation of weak positive features in the 16000 – 20000 cm^{-1} region of the Co^{2+}Cbl + *Lr*PduO/ATP MCD spectrum that are characteristic of five-coordinate $Co^{2+}Cbi^{+}$ (Figure 4A).

As anticipated on the basis of our MCD data in Figure 4, the EPR spectrum of $Co^{2+}Cbi^{+}$ + *Lr*PduO/ATP (Figure 5C) has contributions from two distinct paramagnetic species, an effectively four-coordinate $Co^{2+}Cbi^{+}$ species (responsible for the widely spread resonances in the low-field region) and five-coordinate $Co^{2+}Cbi^{+}$ possessing an axially bound water molecule (see Figure 5B). To obtain a pure spectrum of the four-coordinate $Co^{2+}Cbi^{+}$ fraction, the suitably scaled (×0.5) $Co^{2+}Cbi^{+}$ + *Lr*PduO EPR spectrum (Figure 5B) was subtracted from the composite spectrum in Figure 5C. Although the resulting spectrum (Figure 5D) is qualitatively very similar to that exhibited by the four-coordinate Co^{2+}Cbl fraction bound to the *Lr*PduO/ATP complex (Figure 3D), the $g_{2,3}$ and A(Co) values are in fact somewhat different (Table 3). This result suggests that even though the DMB moiety no longer serves as an axial ligand in the four-coordinate Co^{2+}Cbl + *Lr*PduO/ATP fraction, it nonetheless modulates the geometric and electronic structures of the Co^{2+} center to a small but noticeable degree, presumably via hydrogen-bonding to amino-acid residues near the enzyme active site.

DISCUSSION

LrPduO can adenosylate $Co^{1+}Cbl^{-}$ and $Co^{1+}Cbi$

Thus far, only the CobA-type adenosyltrasferases were believed to participate in the adenosylation of complete as well as incomplete corrinoids (42). However, the kinetic data obtained in this study provide evidence that *in vitro* a PduO-type adenosyltransferase can utilize incomplete corrinoids as alternative substrates, in support of a previous proposal that was based on *in vivo* evidence (32) Interestingly, *Lr*PduO adenosylates $Co^{1+}Cbl^{-}$ and $Co^{1+}Cbi$ with approximately the same catalytic efficiency, as judged on the basis of the similar k_{cat}/K_m values (Table 1). Additionally, under saturating ATP conditions the apparent K_m of *Lr*PduO for $Co^{1+}Cbi$ is nearly identical to that reported for $Co^{1+}Cbl^{-}$ and at least 10-fold lower than for any previously reported adenosyltransferase (32). These results suggest that the nucleotide tail (Figure 1) is relatively unimportant for corrinoid binding to the enzyme active site and for product formation. It is important to note, though, that chemically reduced Co^{1+}corrinoids were used in our activity assays. Thus our kinetic data do not rule out the possibility that the nucleotide tail may be required for allowing the physiological electron donor to accomplish the $Co^{2+} \rightarrow Co^{1+}$corrinoid reduction. However, such a requirement is quite unlikely, based on the close resemblance of our spectroscopic data obtained for Co^{2+}Cbl and $Co^{2+}Cbi^{+}$ bound to the *Lr*PduO/ATP complex (see below) and their obvious similarities with those reported for the CobA adenosyltransferase (28).

NIH-PA Author Manuscript

NIH-PA Author Manuscript

NIH-PA Author Manuscript

Interaction between Co^{2+}corrinoids and LrPduO in the absence of co-subtrate ATP

The fact that the Abs and MCD spectra of Co^{2+}Cbl and $Co^{2+}Cbi^{+}$ change only slightly when *Lr*PduO is added (Figures 2–5) indicates that the geometric and electronic structures of these species are largely preserved in the presence of the enzyme. Nevertheless, small but noticeable changes are observed in each case, signaling that Co^{2+}corrinoid binding to the enzyme active site does occur even in the absence of co-substrate ATP. Specifically, when a solution of Co^{2+}Cbl is incubated with *Lr*PduO, a significant fraction (~30%) of the cofactor converts to the base-off form, in which the Co^{2+} center is axially ligated by a water molecule instead of the DMB moiety (Figure 1) (35). Alternatively, the addition of *Lr*PduO to a solution of $Co^{2+}Cbi^{+}$ causes a small rhombic splitting of the EPR signal (Table 3), possibly reflecting a perturbation of the equatorial ligand environment of the Co^{2+} ion; e.g., via hydrogen-bonding of active-site residues to the peripheral side chains of the corrin macrocycle.

Interaction between Co^{2+}corrinoids and the LrPduO/ATP complex

While the spectroscopic properties of Co^{2+}Cbl and $Co^{2+}Cbi^{+}$ are only weakly affected by the addition of *Lr*PduO, rather drastic spectral changes are observed when the enzyme was pre-incubated with the co-substrate ATP (Figures 2–5). In each case, binding of the Co^{2+}corrinoid substrate to the *Lr*PduO/ATP complex leads to a substantial blue-shift of the dominant Abs feature in the visible spectral region, termed the α-band (Table 2), which corresponds to the lowest-energy corrin-centered $\pi \rightarrow \pi^*$ transition (43–45). Previous studies revealed that the corrin π-based donor orbital involved in this transition also possesses some Co d_{z^2} character, the extent of which is governed by the σ-donor strength of the axial ligand. As a result, the α-band of Co^{2+}corrinoids shifts to higher energy with decreasing electron donating ability of the axial ligand (e.g., from Co^{2+}Cbl to $Co^{2+}Cbi^{+}$, see Table 2) or a weekending of the axial bonding interaction (35, 46).

The large blue-shift of the α-band in response to Co^{2+}Cbl and $Co^{2+}Cbi^{+}$ binding to the *Lr*PduO/ATP complex is accompanied by drastic changes to the corresponding MCD spectra, most notably the appearance of a prominent low-energy feature at ~12340 cm^{-1} (Figures 2 and 4), as well as to their EPR data, in particular a large increase in the g_2, g_3, and A(Co) values (Table 3). Collectively, these spectral perturbations are consistent with a sizeable stabilization of the singly occupied Co $3d_{z^2}$-based molecular orbital (28) owing to a significant weakening of the axial ligand–Co^{2+}corrinoid bonding interaction, so as to generate essentially square-planar Co^{2+} species in the enzyme active site. Although these "activated" forms of Co^{2+}Cbl and $Co^{2+}Cbi^{+}$ bound to the *Lr*PduO/ATP complex are best described as possessing an effectively four-coordinate Co^{2+} center that lacks any significant axial bonding interactions, the corresponding MCD and EPR spectra (Figures 2–5) exhibit small but notable differences. Specifically, when the alternative substrate $Co^{2+}Cbi^{+}$ is used instead of Co^{2+}Cbl, the prominent MCD feature in the near-IR spectral region displays a minor red-shift (by ~30 cm^{-1}, Table 4) and the EPR g and A(Co) values become more rhombic (Table 3). These observations suggest that even though the DMB moiety is displaced from the Co^{2+} ion in the Co^{2+}Cbl + *Lr*PduO/ATP complex, it may still play a role in organizing the enzyme active site for maximum catalytic activity (e.g., by promoting $Co^{2+} \rightarrow Co^{1+}$ reduction).

The spectroscopic data obtained in this work nicely complement the information that has recently been obtained from structural and kinetic studies of *Lr*PduO. First, Mera et al. prepared numerous variants of *Lr*PduO that were characterized by using kinetic and X-ray crystallographic techniques to develop a better understanding of the function of several conserved residues in the enzyme active site (47). Importantly, these studies revealed that substrate inhibition occurs at subsaturating concentrations of ATP, in strong support of an ordered binding scheme according to which the enzyme must bind co-substrate ATP prior to the corrinoid substrate. Second, in the course of this investigation, St. Maurice et al. succeeded

NIH-PA Author Manuscript

NIH-PA Author Manuscript

NIH-PA Author Manuscript

in obtaining an X-ray crystal structure (at 1.9 Å resolution) of Co^{2+}Cbl bound to the *Lr*PduO/ATP complex (48). As expected on the basis of our spectroscopic data reported here, this structure provides visual evidence for the formation of a base-off, four-coordinate Co^{2+}Cbl intermediate in the catalytic cycle of *Lr*PduO. This structure also offers clues as to how the enzyme imposes such a unique coordination environment on the Co^{2+}corrioind substrate. Specifically, it shows that the N-terminus of *Lr*PduO that is disordered in the substrate-free enzyme (32) becomes ordered upon ATP-binding, thereby inducing a distinct active-site conformation that is poised for Co^{2+}corrinoid binding (48). Moreover, a conserved Phe residue moves to within 3.8 Å of the Co^{2+} ion so as to promote dissociation of the axially bound 22 solvent ligand that would normally be present in base-off Co^{2+}Cbl. Although not obvious from the *Lr*PduO crystal structures, our MCD and EPR data indicate that the formation of such a four-coordinate Co^{2+}Cbl intermediate leads to a significant stabilization of the redox-active Co $3d_z2$ orbital that is oriented toward the axial coordination sites, thereby raising the $Co^{2+/1+}$ reduction midpoint potential by an estimated 250 mV (28).

Comparison to other adenosyltransferases

The involvement of unprecedented, essentially four-coordinate Co^{2+}corrinoid intermediates in the catalytic cycles of adenosyltransferases has originally been proposed on the basis of spectroscopic and computational studies of CobA from *Salmonella enterica* and the human enzyme hATR (28,29). As expected by taking into consideration that hATR is a PduO-type adenosyltransferase, Co^{2+}Cbl interacts similarly with this enzyme and *Lr*PduO. Specifically, while binding of Co^{2+}Cbl to hATR in the absence of ATP leads to a partial (~40%) conversion to the base-off form, a significant blue-shift of the α-band and the appearance of the MCD and EPR spectroscopic signatures characteristic of an approximately four-coordinate Co^{2+}corrinoid species are observed when hATR was pre-incubated with co-substrate ATP (29). However, the prominent low-energy feature in the MCD spectrum of Co^{2+}Cbl + hATR/ATP is blue-shifted by 240 cm^{-1} relative to that of Co^{2+}Cbl + *Lr*PduO/ATP (Table 4), signifying a slightly stronger residual axial bonding interaction in the former species. Moreover, a comparison of the corresponding EPR spectra reveals that the conversion from the five- to the four-coordinate Co^{2+}Cbl species is more complete in the case of hATR (~90%) than for *Lr*PduO (~40%). Collectively, these results suggest that a stronger interaction could exist between the dissociated DMB moiety of the "activated" Co^{2+}Cbl species and the enzyme active site in hATR than in *Lr*PduO. It is tempting to speculate, then, that due to this increased interaction with the nucleotide loop, hATR may exhibit an increased substrate specificity and thus be unable to adenosylate incompletely assembled corrinoids, such as $Co^{2+}Cbi^{+}$. Although to our knowledge the range of possible corrinoid substrates for hATR has not yet been established, it is interesting to note that the PduO-type adenosyltransferase from *S. enterica* appears to be specific for AdoCbl synthesis, despite its high sequence similarity with *Lr*PduO (49).

In the case of CobA, for which the natural substrate is a Co^{2+}Cbl precursor that lacks the nucleotide loop and thus more closely resembles $Co^{2+}Cbi^{+}$ (16,50), MCD and EPR spectroscopic studies revealed that in the $Co^{2+}Cbi^{+}$ + CobA/ATP complex, a predominant fraction (~70%) of four-coordinate Co^{2+}corrinoid species is formed (28). When the alternative substrate Co^{2+}Cbl is added to the CobA/ATP complex, however, the conversion to a similar four-coordinate Co^{2+} species is largely suppressed (to ~10%). While hATR and CobA are thus relatively specific for their respective substrates, the results obtained in this study reveal that a sizeable a fraction of a four-coordinate Co^{2+}corrinoid species is formed regardless of whether Co^{2+}Cbl or $Co^{2+}Cbi^{+}$ binds to the *Lr*PduO/ATP complex (40% and 50%, respectively). Although this low substrate-specificity of *Lr*PduO is consistent with our kinetic data reported in the *Results and Analysis* section (Table 1), this finding is rather unexpected, because among the three types of adenosyltransferases found in *Salmonella enterica*, CobA has been presumed

NIH-PA Author Manuscript

NIH-PA Author Manuscript

NIH-PA Author Manuscript

to be the only enzyme capable of adenosylating incomplete corrionid species (7,8,16,28). Yet, the nearly identical positions of the prominent near-IR features in the MCD spectra of $Co^{2+}Cbi^{+}$ + *Lr*PduO/ATP and $Co^{2+}Cbi^{+}$ + CobA/ATP (Table 4) suggest that $Co^{2+}Cbi^{+}$ does in fact interact similarly with the *Lr*PduO/ATP and CobA/ATP complexes. Despite these similarities, a more complete conversion to a four-coordinate $Co^{2+}Cbi^{+}$ species occurs in the latter enzyme (50% and 70% for *Lr*PduO and CobA, respectively).

Although small differences exist among the spectroscopic signatures of the formally four-coordinate Co^{2+}corrinoid species that have now been identified in the active sites of various adenosyltransferases (28,29), the general strategy of these enzymes evidently involves the formation of an essentially square-planar Co^{2+}corrinoid intermediate, so as to reduce the thermodynamic barrier for the reduction to the Co^{1+} state through stabilization of the redox-active, Co $3d_z2$-based molecular orbital that is oriented along the axial coordination sites of the Co^{2+} ion. Remarkably, for each adenosyltransferase studied to date (28,29), this “activated” Co^{2+}corrinoid intermediate is formed in high yield only in the presence of co-substrate ATP, which provides a mechanism for protecting the enzyme active site from being attacked by the transiently formed Co^{1+}corrinoid “supernucleophile”. Collectively, the insights gained in this study and the recent structural and kinetic characterizations of *Lr*PduO provide an excellent basis for further investigations into the fascinating bio-organometallic reaction catalyzed by PduO-type adenosyltransferases.

References

1. Butler, PA.; Kräutler, B. Topics in organometallic chemistry. 17. Springer; Berlin, Heidelberg: 2006.
2. Lenhert PG. The structure of vitamin B_{12} VII. The X-ray analysis of the vitamin B_{12} coenzyme. Proceedings of the Royal Society of London Series A 1968;303:45–84.
3. Chowdhury S, Banerjee R. Role of the dimethylbenzimidazole tail in the reaction catalyzed by coenzyme B_{12}-dependent methylmalonyl-CoA mutase. Biochemistry 1999;38:15287–15294. [PubMed: 10563814]
4. Banerjee R. Radical peregrinations catalyzed by coenzyme B_{12}-dependent enzymes. Biochemistry 2001;40:6191–6198. [PubMed: 11371179]
5. Chowdhury S, Banerjee R. Thermodynamic and kinetic characterization of Co–C bond homolysis catalyzed by coenzyme B_{12}-dependent methylmalonyl-CoA mutase. Biochemistry 2000;39:7998–8006. [PubMed: 10891081]
6. Marsh ENG, Ballou DP. Coupling of cobalt-carbon bond homolysis and hydrogen atom abstraction in adenosylcobalamin-dependent glutamate mutase. Biochemistry 1998;37:11864–11872. [PubMed: 9718309]
7. Johnson CLV, Pechonick E, Park SD, Havemann GD, Leal NA, Bobik TA. Functional genomic, biochemical, and genetic characterization of the *Salmonella* pduO gene, an ATP:cob(I)alamin adenosyltransferase gene. J Bacteriol 2001;183:1577–1584. [PubMed: 11160088]
8. Buan NR, Suh S-J, Escalante-Semerena JC. The eutT gene of *Salmonella enterica* encodes an oxygen-labile, metal-containing ATP:corrinoid adenosyltransferase enzyme. J Bacteriol 2004;186:5708–5714. [PubMed: 15317775]
9. Thoma NH, Evans PR, Leadlay PF. Protection of radical intermediates at the active site of adenosylcobalamin-dependent methylmalonyl-CoA mutase. Biochemistry 2000;39:9213–9221. [PubMed: 10924114]
10. Gerfen GJ, Licht S, Willems J-P, Hoffman BM, Stubbe J. Electron paramagnetic resonance investigations of a kinetically competent intermediate formed in ribonucleotide reduction: evidence for a thiyl radical-cob(II)alamin interaction. J Am Chem Soc 1996;118:8192–8197.
11. Brown KL, Zou X. Thermolysis of coenzymes B_{12} at physiological temperatures: activation parameters for cobalt–carbon bond homolysis and a quantitative analysis of the perturbation of the homolysis equilibrium by the ribonucleoside triphosphate reductase from *Lactobacillus leichmannii*. Journal of Inorganic Biochemistry 1999;77:185–195. [PubMed: 10643658]

NIH-PA Author Manuscript NIH-PA Author Manuscript NIH-PA Author Manuscript

12. Banerjee R. Radical carbon skeleton rearrangements: catalysis by coenzyme B_{12}-dependent mutases. Chem Rev 2003;103:2083–2094. [PubMed: 12797824]
13. Banerjee R, Ragsdale SW. The many faces of vitamin B_{12}: catalysis by cobalamin-dependent enzymes. Annu Rev Biochem 2003;72:209–247. [PubMed: 14527323]
14. Marsh ENG, Drennan CL. Adenosylcobalamin-dependent isomerases: new insight into structure and mechanism. Curr Opin Chem Biol 2001;5:499–505. [PubMed: 11578922]
15. Fenton WA, Rosenberg LE. The defect in the CblB class of human methylmalonic aciduria: deficiency of cob(I)alamin adenosyltransferase activity in extracts of cultured fibroblasts. Biochemical and Biophysical Research Communications 1981;98:283–289. [PubMed: 7213387]
16. Escalante-Semerena JC, Suh S-J, Roth JR. CobA function is required for both de novo cobalamin biosynthesis and assimilation of exogenous corrinoids in *Salmonella typhimurium*. J Bacteriol 1990;172:273–280. [PubMed: 2403541]
17. Dobson CM, Wai T, Leclerc D, Kadir H, Narang M, Lerner-Ellis JP, Hudson TJ, Rosenblatt DS, Gravel RA. Identification of the gene responsible for the cblB complementation group of vitamin B_{12}-dependent methylmalonic aciduria. Hum Mol Gen 2002;11:3361–3369. [PubMed: 12471062]
18. Warren MJ, Raux E, Schubert HL, Escalante-Semerena JC. The biosynthesis of adenosylcobalamin (vitamin B_{12}). Natural Product Reports 2002;19:390–412. [PubMed: 12195810]
19. Walker GA, Murphy S, Huennekens FM. Enzymatic conversion of vitamin B_{12a} to adenosyl-B_{12}: evidence for the existence of two separate reducing systems. Arch Biochem Biophysics 1969;134:95–102.
20. Lawrence AD, Deery E, McLean KJ, Munro AW, Pickersgill RW, Rigby SE, Warren MJ. Identification, characterization and structure/function analysis of a corrin reductase involved in adenosylcobalamin biosynthesis. J Biol Chem. 2008in press
21. Fonseca MV, Escalante-Semerena JC. Reduction of cob(III)alamin to cob(II)alamin in *Salmonella enterica Serovar Typhimurium* LT2. J Bacteriol 2000;182:4304–4309. [PubMed: 10894741]
22. Olteanu H, Wolthers KR, Munro AW, Scrutton NS, Banerjee R. Kinetic and thermodynamic characterization of the common polymorphic variants of human methionine synthase reductase. Biochemistry 2004;43:1988–1997. [PubMed: 14967039]
23. Lexa D, Saveant J-M. The electrochemistry of vitamin B_{12}. Acc Chem Res 1983;16:235–243.
24. Mciver L, Leadbeater C, Campopiano DJ, Baxter RL, Daff SN, Chapman SK, Munro AW. Characterisation of flavodoxin $NADP^+$ oxidoreductase and flavodoxin; key components of electron transfer in *Escherichia coli*. Eur J Biochem 1998;257:557–585.
25. Fonseca MV, Escalante-Semerena JC. An *in vitro* reducing system for the enzymic conversion of cobalamin to adenosylcobalamin. J Biol Chem 2001;276:32101–32108. [PubMed: 11408479]
26. Sampson EM, Johnson CLV, Bobik TA. Biochemical evidence that the pduS gene encodes a bifunctional cobalamin reductase. Microbiology 2005;151:1169–1177. [PubMed: 15817784]
27. Leal NA, Olteanu H, Banerjee R, Bobik TA. Human ATP:cob(I)alamin adenosyltransferase and its interaction with methionine synthase reductase. J Biol Chem 2004;279:47536–47542. [PubMed: 15347655]
28. Stich TA, Buan NR, Escalante-Semerena JC, Brunold TC. Spectroscopic and computational studies of the ATP:corrinoid adenosyltransferase (CobA) from *Salmonella enterica*: insights into the mechanism of adenosylcobalamin biosynthesis. J Am Chem Soc 2005;127:8710–8719. [PubMed: 15954777]
29. Stich TA, Yamanishi M, Banerjee R, Brunold TC. Spectroscopic evidence for the formation of a four-coordinate Co^{2+}cobalamin species upon binding to the human ATP:cobalamin adenosyltransferase. J Am Chem Soc 2005;127:7660–7661. [PubMed: 15913339]
30. Leal NA, Park SD, Kima PE, Bobik TA. Identification of the human and bovine ATP:cob(I)alamin adenosyltransferase cDNAs based on complementation of a bacterial mutant. J Biol Chem 2003;278:9227–9234. [PubMed: 12514191]
31. Dobson CM, Wai T, Leclerc D, Wilson A, Wu X, Dore C, Hudson T, Rosenblatt DS, Gravel RA. Identification of the gene responsible for the cblA complementation group of vitamin B_{12}-responsive methylmalonic aciduria based on analysis of prokaryotic gene arrangements. Proc Natl Acad Sci USA 2002;99:15554–15559. [PubMed: 12438653]

NIH-PA Author Manuscript

NIH-PA Author Manuscript

NIH-PA Author Manuscript

32. StMaurice M, Mera PE, Taranto MP, Sesma F, Escalante-Semerena JC, Rayment I. Structural characterization of the active site of the PduO-type ATP:co(I)rrinoid adenosyltransferase from *Lactobacillus reuteri*. J Biol Chem 2007;282:2596–2605. [PubMed: 17121823]
33. Rocco CJ, Dennison KL, Klenchin VA, Rayment I, Escalante-Semerena JC. Construction and use of new cloning vectors for the rapid isolation of recombinant proteins from *Escherichia coli*. Plasmid. 2008in press
34. Neese, F. (1997), University of Konstanz.
35. Stich TA, Buan NR, Brunold TC. Spectroscopic and computational studies of Co^{2+}corrinoids: spectral and electronic properties of the biologically relevant base-on and base-off forms of Co^{2+}cobalamin. J Am Chem Soc 2004;126:9735–9749. [PubMed: 15291577]
36. Pilbrow, JR. B_{12}. Dolphin, D., editor. Wiley; New York: 1982. p. 431-462.
37. Doorslaer SV, Jeschke G, Epel B, Goldfarb D, Eichel R-A, Kräutler B, Schweiger A. Axial solvent coordination in “base-off” cob(II)alamin and related Co(II)-corrinates revealed by 2D-EPR. J Am Chem Soc 2003;125:5915–5927. [PubMed: 12733932]
38. Johnson, MK. Physical methods in bioinorganic chemistry. Lawrence Que, J., editor. University Science Books; Sausalito: 2000. p. 233-285.
39. Schellman JA. Circular dichroism and optical rotation. Chem Rev 1975;75:323–331.
40. Ozarowski A, Lee HM, Balch AL. Crystal environments probed by EPR spectroscopy. Variations in the EPR spectra of Co^{II}(octaethylporphyrin) doped in crystalline diamagnetic hosts and a reassessment of the electronic structure of four-coordinate cobalt(II). J Am Chem Soc 2003;125:12606–12614. [PubMed: 14531705]
41. Assour JM, Kahn WK. Electron spin resonance of α- and β-cobalt phthalocyanine. J Am Chem Soc 1965;87:207–212.
42. Suh S-J, Escalante-Semerena JC. Purification and initial characterization of the ATP:corrinoid adenosyltransferase encoded by the cobA gene of *Salmonella typhimurium*. J Bacteriol 1995;177:921–925. [PubMed: 7860601]
43. Kuhn H, Drexhage KH, Martin H. The light absorption of vitamin B_{12}. Proceedings of the Royal Society of London Series 1965;A288:348–351.
44. Firth RA, Hill HAO, Pratt JM, Williams RJP, Jackson WR. The 31 circular dichroism and absorption spectra of some vitamin B_{12} derivatives. Biochemistry 1967;6:2178–2189. [PubMed: 6049452]
45. Day P. A theory of the optical properties of vitamin B_{12} and its derivatives. Theoret Chim Acta 1967;7:328–341.
46. Stich TA, Brooks AJ, Buan NR, Brunold TC. Spectroscopic and computational studies of Co^{3+}-corrinoids: spectral and electronic properties of the B_{12} cofactors and biologically relevant precursors. J Am Chem Soc 2003;125:5897–5914. [PubMed: 12733931]
47. Mera PE, StMaurice M, Rayment I, Escalante-Semerena JC. Structural and functional analyses of the human-type corrinoid adenosyltransferase (PduO) from *Lactobacillus reuteri*. Biochemistry 2007;46:13829–13836. [PubMed: 17988155]
48. StMaurice M, Mera PE, Park K, Brunold TC, Escalante-Semerena JC, Rayment I. Structural characterization of a human-type corrinoid adenosyltransferase confirms that coenzyme B_{12} is synthesized through a four-coordinate intermediate. Biochemistry. 2008submitted
49. Johnson CL, Pechonick E, Park SD, Havemann GD, Leal NA, Bobik TA. Functional genomic, biochemical, and genetic characterization of the *SalmonellapduO* gene, an ATP:cob(I)alamin adenosyltransferase gene. J Bacteriol 2001;183:1577–1584. [PubMed: 11160088]
50. O’Toole GA, Escalante-Semerena JC. cobU-dependent assimilation of nonadenosylated cobinamide in cobA mutants of *Salmonella typhimurium*. J Bacteriol 1993;175:6328–6336. [PubMed: 8407805]

NIH-PA Author Manuscript

NIH-PA Author Manuscript

NIH-PA Author Manuscript

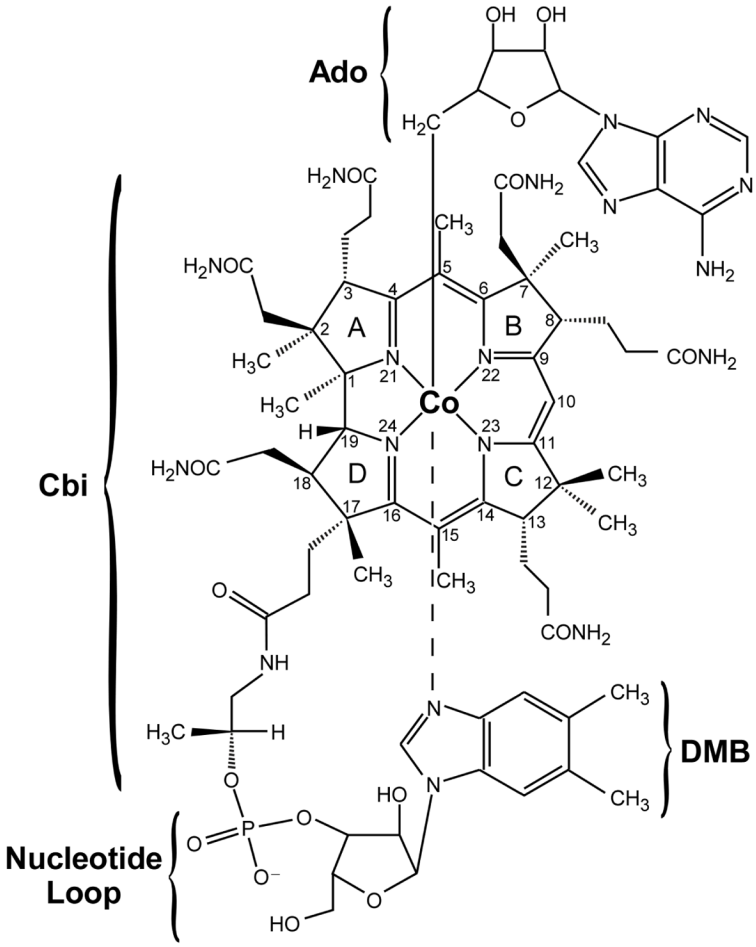

Figure 1.
Schematic representation of the adenosylcobalamin cofactor (AdoCbl). In adenosylcobinamide ($AdoCbi^+$), the nucleotide loop including the DMB base is absent and a water molecule occupies the lower axial position.

NIH-PA Author Manuscript

NIH-PA Author Manuscript

NIH-PA Author Manuscript

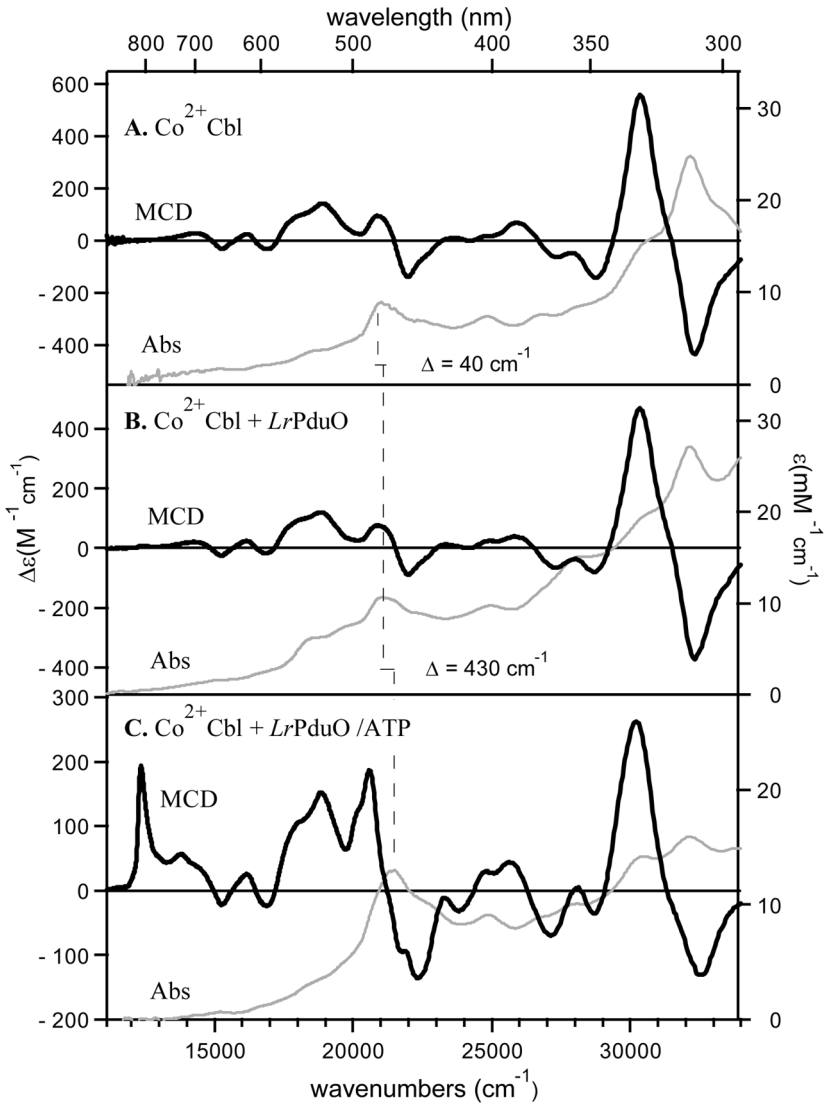

Figure 2.

Abs (gray traces, right axis) and 7 T MCD (black traces, left axis) spectra collected at 4.5 K of (A) free Co^{2+}Cbl, (B) Co^{2+}Cbl in the presence of *Lr*PduO, and (C) Co^{2+}Cbl in the presence of the *Lr*PduO/ATP complex. The peak position of the dominant Abs feature (the α-band) is indicated by the vertical solid line.

NIH-PA Author Manuscript

NIH-PA Author Manuscript

NIH-PA Author Manuscript

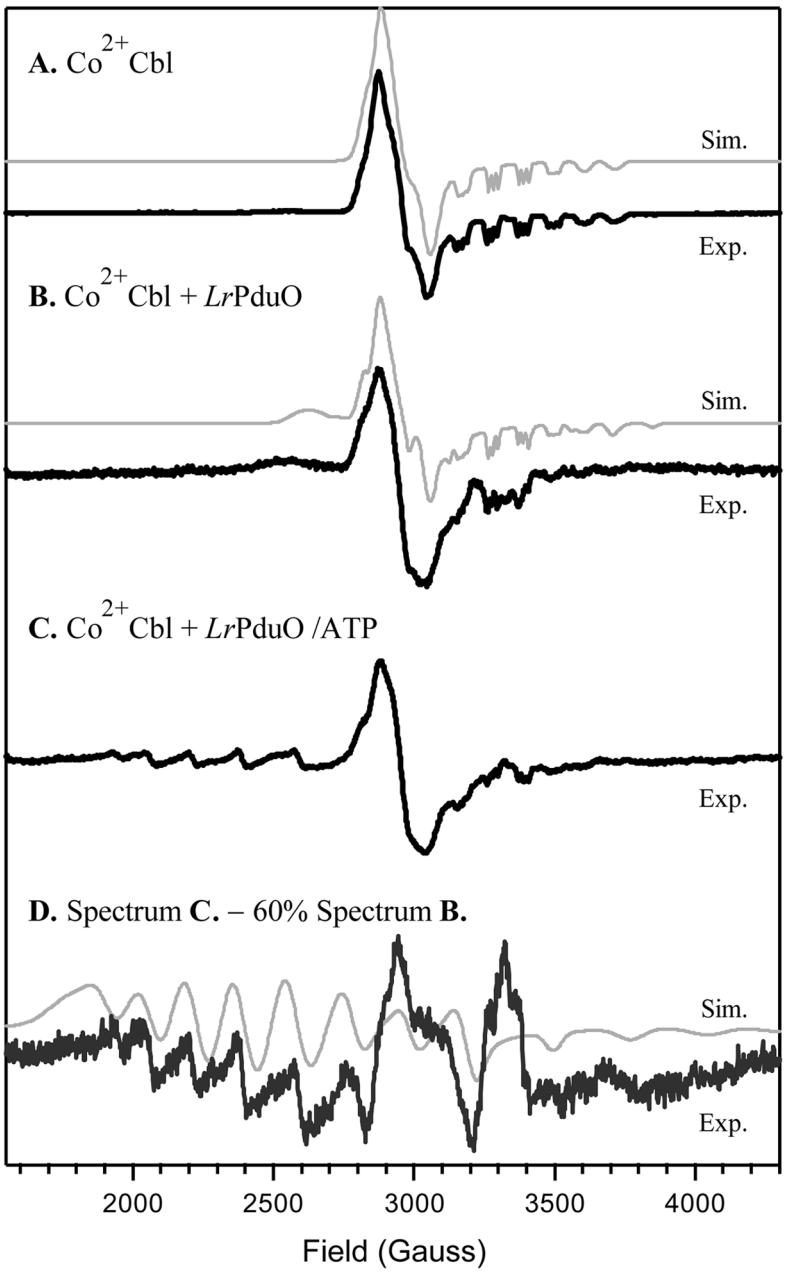

Figure 3.

EPR spectra collected at 20 K of (A) free Co^{2+}Cbl, (B) Co^{2+}Cbl in the presence of *Lr*PduO, and (C) Co^{2+}Cbl in the presence of the *Lr*PduO/ATP complex. Spectrum D was obtained by subtracting 60% of spectrum B from spectrum C. Spectral simulations (thin lines) were performed using the parameters provided in Table 3.

NIH-PA Author Manuscript

NIH-PA Author Manuscript

NIH-PA Author Manuscript

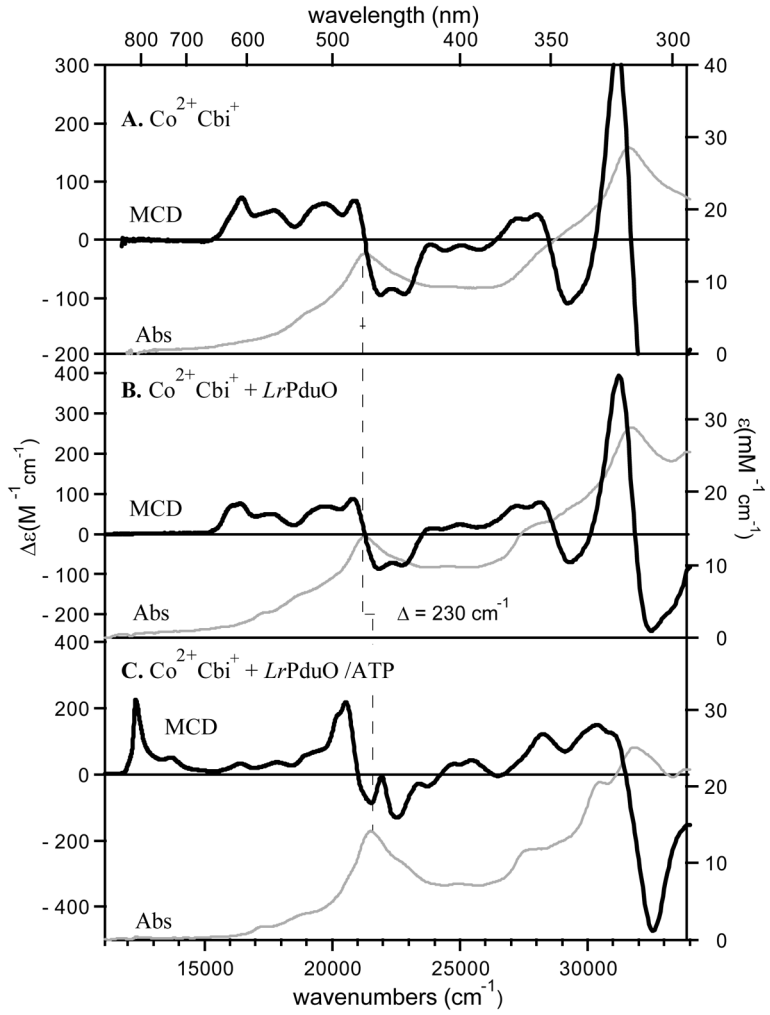

Figure 4.

Abs (gray traces, right axis) and 7 T MCD (black traces, left axis) spectra collected at 4.5 K of (A) free $Co^{2+}Cbi^{+}$, (B) $Co^{2+}Cbi^{+}$ in the presence of *Lr*PduO, and (C) $Co^{2+}Cbi^{+}$ in the presence of the *Lr*PduO/ATP complex. The peak position of the dominant Abs feature (the α-band) is indicated by the vertical solid line.

NIH-PA Author Manuscript
NIH-PA Author Manuscript
NIH-PA Author Manuscript

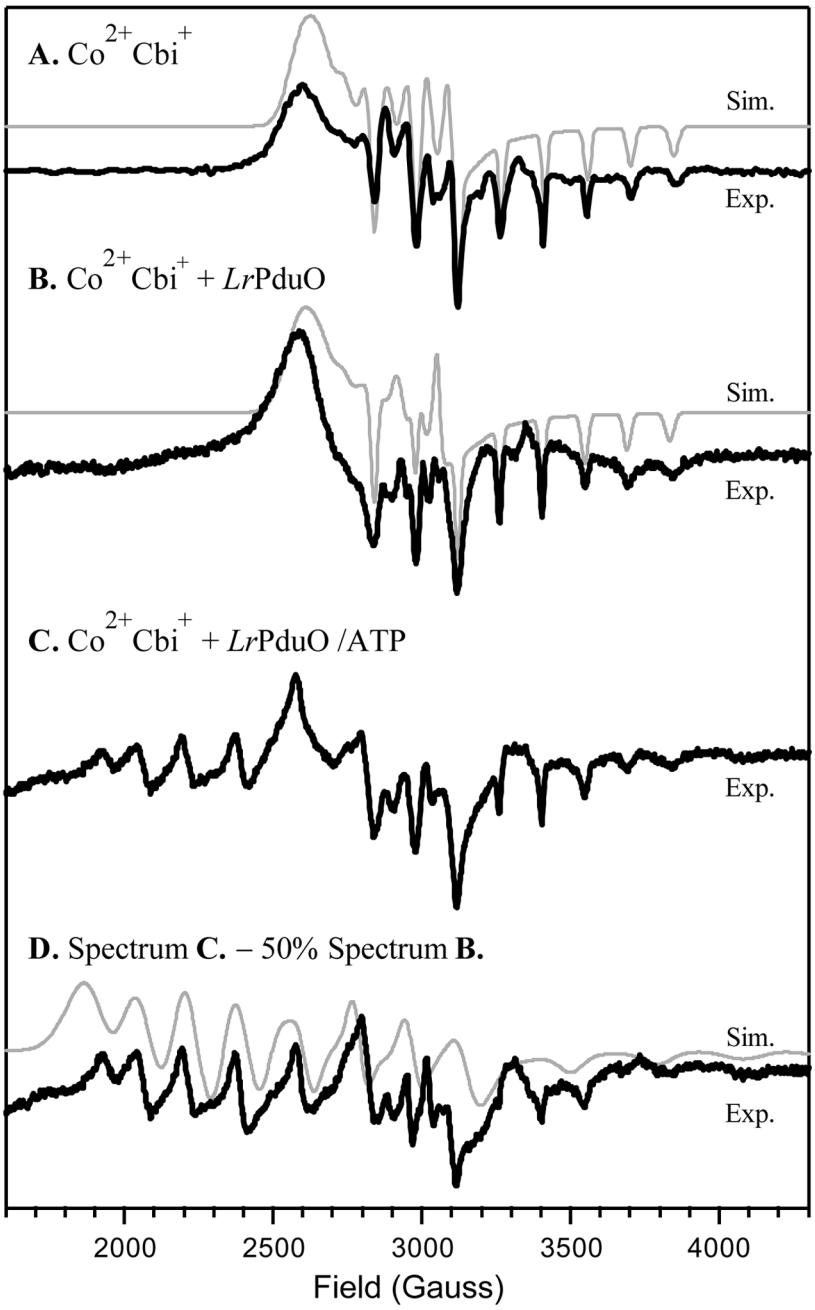

Figure 5.

EPR spectra collected at 20 K of (A) free $Co^{2+}Cbi^{+}$, (B) $Co^{2+}Cbi^{+}$ in the presence of *Lr*PduO, and (C) $Co^{2+}Cbi^{+}$ in the presence of the *Lr*PduO/ATP complex. Spectrum D was obtained by subtracting 50% of spectrum B from spectrum C. Spectral simulations (thin lines) were performed using the parameters provided in Table 3.

NIH-PA Author Manuscript

NIH-PA Author Manuscript

NIH-PA Author Manuscript

Table 1

Kinetic parameters for the *Lr*PduO catalyzed conversion of $Co^{1+}Cbl^{-}$ and $Co^{1+}Cbi$ to AdoCbl and $AdoCbi^{+}$, respectively[a]

Substrate	kcat (s^{-1})	Km (μM)	kcat/Km (M^{-1} s^{-1})
$Co^{1+}Cbl^{-}$	$2.4 \pm 0.1 \times 10^{-2}$	$13 \pm 1 \times 10^{-2}$	$1.8 \pm 0.2 \times 10^{5}$
$Co^{1+}Cbi$	$2.0 \pm 0.2 \times 10^{-2}$	$9.6 \pm 1.4 \times 10^{-2}$	$2.1 \pm 0.4 \times 10^{5}$

[a] Data for $Co^{1+}Cbl^{-}$ were taken from ref (32).

NIH-PA Author Manuscript

NIH-PA Author Manuscript

NIH-PA Author Manuscript

Table 2

Changes in the α-band positions of Co^{2+}Cbl and $Co^{2+}Cbi^{+}$ caused by the addition of *Lr*PduO in the absence and presence of co-substrate ATP, as determined from the 4.5 K Abs spectra in Figures 2 and 4[a]

Species	Free Corrinoid	+ *Lr*PduO	+ *Lr*PduO/ATP
Co^{2+}Cbl	21010 cm^{-1} (476.0 nm)	21050 cm^{-1} (475.0 nm)	21480 cm^{-1} (465.5 nm)
$Co^{2+}Cbi^{+}$	21250 cm^{-1} (470.5 nm)	21250 cm^{-1} (470.5 nm)	21480 cm^{-1} (465.5 nm)

[a] Note that a blue-shift of the α-band reflects a weakening of the axial ligand–Co^{2+}corrinoid bonding interaction.

NIH-PA Author Manuscript
NIH-PA Author Manuscript
NIH-PA Author Manuscript

Table 3

EPR g Values and ^{59}Co Hyperfine Values A(Co) (in MHz) from the spectral simulations presented in Figures 3 and 5

Species	Spectrum[a]	g_1	g_2	g_3	A_1(Co)	A_2(Co)	A_3(Co)
Free Co^{2+}Cbl [b]	3A	2.00	2.23	2.28	305	30	40
Co^{2+}Cbl + *Lr*PduO [c]	3B	2.00	2.23	2.28	305	30	40
		2.00	2.34	2.37	400	220	220
Co^{2+}Cbl + *Lr*PduO/ATP	3D	1.99	2.70	2.72	770	755	595
Free Co^{2+}Cbi$^+$ [b]	5A	2.00	2.34	2.34	405	220	220
Co^{2+}Cbi$^+$ + *Lr*PduO	5B	2.00	2.34	2.37	400	220	220
Co^{2+}Cbi$^+$ + *Lr*PduO/ATP	5D	1.99	2.65	2.74	810	665	565

[a] The labels refer to the spectra in Figures 3 and 5.

[b] From ref (28).

[c] This spectrum has contributions from ~70% base-on and ~30% base-off Co^{2+}Cbl.

NIH-PA Author Manuscript

NIH-PA Author Manuscript

NIH-PA Author Manuscript

Table 4

Peak position of the prominent MCD feature in the near-IR spectral region observed for Co^{2+}corrinoids bound to several alkyltransferase/ATP complexes

Co^{2+}Cbl + *Lr*PduO/ATP	**$Co^{2+}Cbi^{+}$ + *Lr*PduO/ATP**	**$Co^{2+}Cbi^{+}$ + CobA/ATP[a]**	**Co^{2+}Cbl + hATR/ATP[b]**
12340 cm^{-1} (810.0 nm)	12310 cm^{-1} (812.5 nm)	12340 cm^{-1} (810 nm)	12580 cm^{-1} (795 nm)

[a] From ref (28).

[b] From ref (29).